Published in final edited form as:
J Nucl Med. 2010 June ; 51(6): 942–950. doi:10.2967/jnumed.109.071290.

Preparation, biological evaluation and pharmacokinetics of human anti-HER1 monoclonal antibody, Panitumumab, labeled with ^{86}Y for quantitative PET imaging of carcinoma

Tapan K. Nayak[*], **Kayhan Garmestani**, **Kwamena E. Baidoo**, **Diane E. Milenic**, and **Martin W. Brechbiel**[*]
Radioimmune & Inorganic Chemistry Section, Radiation Oncology Branch, National Cancer Institute, National Institute of Health, Bethesda, MD-20892, USA

Abstract

Purpose—Panitumumab, a human monoclonal antibody (mAb) that binds to the epidermal growth factor receptor (EGFR/HER1), was approved by the FDA in 2006 for the treatment of patients with HER1-expressing carcinoma. In this report, we describe preclinical development of ^{86}Y-CHX-A″-DTPA-panitumumab for quantitative positron emission tomography (PET) imaging of HER1-expressing carcinoma.

Experimental design—Panitumumab was conjugated to CHX-A″-DTPA and radiolabeled with ^{86}Y. *In vivo* biodistribution, PET imaging, blood clearance, area under the curve (AUC), area under the moment curve (AUMC) and mean residence time (MRT) were determined on mice bearing HER1-expressing human colorectal (LS-174T), prostate (PC-3) and epidermoid (A431) tumor xenografts. Receptor-specificity was demonstrated by co-injection of 0.1 mg panitumumab with the radioimmunoconjugate (RIC).

Results—^{86}Y-CHX-A″-DTPA-panitumumab was routinely prepared with a specific activity exceeding 2 GBq/mg. Biodistribution and PET imaging studies demonstrated high HER1-specific tumor uptake of the RIC. In mice bearing LS-174T, PC-3 or A431 tumors, the tumor uptake at 3 d were 34.6 ± 5.9, 22.1± 1.9 and 22.7 ± 1.7 % ID/g, respectively. The corresponding tumor uptake in mice co-injected with 0.1 mg panitumumab was 9.3 ± 1.5, 8.8 ± 0.9 and 10.0 ± 1.3 % ID/g, respectively at the same time point, demonstrating specific blockage of the receptor. Normal organ and tumor uptake quantified by PET were closely related (r^2= 0.95) to values determined by biodistribution studies. LS-174T tumor had the highest AUC (96.8 ± 5.6 %ID.d.g^{-1}) and AUMC (262.5 ± 14.9 %ID.d^2.g^{-1}), however the tumor MRT were identical for all three tumors (2.7–2.8 d).

Conclusion—This study demonstrates the potential of ^{86}Y-CHX-A″-DTPA-panitumumab for quantitative non-invasive PET imaging of HER1-expressing tumors, and represents the first step towards clinical translation.

Keywords

PET imaging; HER1; Panitumumab; immunoPET; ^{86}Y

[*]Corresponding author and reprint requests: Dr. Martin W. Brechbiel or Dr. Tapan K. Nayak, 10 Center Drive MSC-1002, Building 10, Room B3B69, Bethesda, Bethesda, MD 20892. Fax: 301-402-1923. martinwb@mail.nih.gov.
First author (Post-doctoral fellow): Tapan K. Nayak, 10 Center Drive MSC-1002, Building 10, Room B3B69, Bethesda, Bethesda, MD 20892. Fax: 301-402-1923. tapann@gmail.com

Authors declare no conflict of interests.

Introduction

The epidermal growth factor receptor (EGFR/HER1/Erb1) is a transmembrane glycoprotein belonging to subclass I of the tyrosine kinase receptor superfamily (1,2). HER1 signaling is firmly regulated in normal cells. The receptor is over-expressed in cancers ranging from lung to colorectal because of HER1 gene amplification and anomalous expression and signaling in cancer cells. Over-expression of the receptor is associated with poor survival, disease progression and resistance to conventional chemotherapy (1,2). To overcome resistance to chemotherapy and improve outcomes, HER1-targeted therapies are actively being developed. Two major classes of clinical therapies have been explored in the treatment of HER1-expressing cancer with moderate success (3,4). These are anti-HER1 monoclonal antibodies (mAbs) and HER1-specific tyrosine kinase inhibitors. Currently, two mAbs, cetuximab and panitumumab, are FDA approved.

Cetuximab (Erbitux®) is a chimeric anti-HER1 IgG_1-isotype mAb indicated for use in patients with HER1-expressing metastatic colorectal cancer as a single-agent immunotherapy or in combination with irinotecan-based chemotherapy (3,4). The anti-tumor activity of cetuximab, however, requires high doses and adverse reactions related to immune response and hypersensitivity to the antibody have been reported in ~19% of patients with 3% of the patients experiencing severe reactions (4–6). The fully human anti-HER1 mAb, panitumumab (Vectibix®), was developed using XenoMouse technology with the objective of improving therapeutic efficacy and decreasing the potential of eliciting immune responses in patients (7). Panitumumab binds to the ligand binding domain (domain III) of HER1 and is rapidly internalized leading to down-regulation of cell surface HER1 *in vitro* and *in vivo* (7,8). In addition to inhibition the of phosphorylation of HER1 and MAPK/Akt, panitumumab also causes cell cycle arrest and inhibits tumor growth by suppressing the production of pro-angiogenic factors such as VEGF and IL-8 by tumor cells (7,8).

Panitumumab was approved by the FDA in 2006 for treatment of patients with HER1-expressing, metastatic colorectal carcinoma with disease progression on or following fluoropyrimidine-, oxiplatin-, and irinotecan-containing chemotherapy regimens (9–11). Panitumumab therapy is well tolerated in patients (12,13). A phase III trial of 463 patients with refractory metastatic colorectal cancer compared panitumumab plus best supportive care (BSC) versus BSC. In the panitumumab group, 46 % reduction in tumor progression rate was reported as compared with BSC alone (14). Panitumumab also significantly improved progression-free survival with manageable toxicity and was efficient in time-related end-points. The clinical efficacy of panitumumab is currently being evaluated in patients with other types of cancers such as lung, breast, renal, head and neck and ovarian cancers (10).

A critical factor in screening patients for targeted therapy is evaluating the presence and the amount of the specific target in the tumor, and its relevance to the disease state. Initial clinical experience with both cetuximab and panitumumab therapy revealed that HER1 levels detected by immunohistochemistry did not correlate with response to anti-HER1 immunotherapy (15, 16). Along with other pathological procedures and tests, non-invasive nuclear imaging is often used to assess the status of the specific target. For instance, to assess the status of HER1-expression and cetuximab distribution, cetuximab has been radiolabeled with radionuclides such as ^{99m}Tc and ^{111}In for single photon emission computerized tomography (SPECT) imaging (17–20) while cetuximab radiolabeled with ^{64}Cu and ^{89}Zr have been explored for positron emission tomography (PET) (21–24). Panitumumab binds to a different epitope of HER1 than cetuximab; therefore, there is a need to develop a panitumumab-specific imaging agent. An extensive pre-clinical evaluation has been performed in this laboratory with panitumumab conjugated with CHX-A″-DTPA and radiolabeled with ^{111}In (25). In that report, conjugating 1–2 molecules of CHX-A″-DTPA to panitumumab did not alter the binding

affinity of panitumumab. Panitumumab was found to retain reactivity with HER1 following modification with the CHX-A″-DTPA ligand and when radiolabeled with ^{111}In. Excellent tumor targeting by ^{111}In-CHX-A″-DTPA-panitumumab was demonstrated *in vivo* by direct quantitation of tumors and normal tissues in five tumor xenograft models. Considering the superiority of PET over single photon scintigraphy, the development of a panitumumab-specific PET RIC was deemed a worthwhile pursuit.

Of the numerous longer-lived positron-emitting radionuclides available such as ^{124}I, ^{86}Y, ^{64}Cu and ^{89}Zr for radioimmunoimaging, we selected ^{86}Y due to its appropriate half-life (14.7 h), suitability for internalizing mAbs, well-established chemistry, and availability (26,27). In addition to these attractive features, ^{86}Y can also serve as a surrogate marker for ^{90}Y based radioimmunotherapy (RIT) and peptide receptor radionuclide therapy (PRRT) (28,29). At the time of manuscript preparation, a study describing ^{64}Cu-DOTA-panitumumab was *in press* (30). In this study, ^{64}Cu-DOTA-panitumumab was successfully used to image HER1-expressing head and neck squamous cell tumor xenografts in mice.

In the present study, the preparation and evaluation of ^{86}Y-CHX-A″-DTPA-panitumumab for potential use in risk stratification and quantitative non-invasive imaging of HER1 and assessment of panitumumab uptake in pre-clinical cancer models is described. To achieve this objective, ^{86}Y-CHX-A″-DTPA-panitumumab was assessed by *in vivo* biodistribution, PET imaging and quantification, blood pharmacokinetics, along with detailed analysis of area under the curve (AUC), area under the moment curve (AUMC) and mean residence time (MRT) with mice bearing HER1-expressing human colorectal (LS-174T), prostate (PC-3) and epidermoid (A431) tumor xenografts.

Methods and Materials

Preparation of ^{86}Y-CHX-A″-DTPA-Panitumumab

Production and purification of ^{86}Y—^{86} Y was produced by the previously described ^{86}Sr(p,n)^{86}Y reaction, with minor modifications in the post-irradiation processing of the $SrCO_3$ target (27). Briefly, the post-irradiated $SrCO_3$ target was dissolved in 500 μL of 3 M ultrapure grade nitric acid and heated to dryness twice; 300 μL of 8 M ultrapure grade nitric acid was added to the residue to dissolve ^{86}Y. The mixture was allowed to cool in an ice bath to precipitate the Sr. The supernatant containing ^{86}Y was separated and heated to dryness. The ^{86}Y was extracted with 2 × 300 μL 3 M nitric acid and loaded onto a pre-equilibrated 0.5 mL bed volume of Sr resin (EiChrom Industries, Darien, IL, USA), and eluted with 3 M nitric acid. The eluted ^{86}Y solution was heated to dryness and the resultant ^{86}Y residue was extracted with 3 × 200 μL 2 M nitric acid and loaded onto a pre-conditioned Y-selective RE-Spec resin column (EiChrom Industries, Darien, IL, USA). The ^{86}Y was eluted with 2 M nitric acid. The eluate containing ^{86}Y was heated to dryness, and the ^{86}Y residue was dissolved in 0.1 M nitric acid for radiolabeling procedures.

Radiolabeling CHX-A″-DTPA-Panitumumab with ^{86}Y—The bifunctional chelate, CHX-A″-DTPA, was conjugated to panitumumab as previously described (25). The chelate to protein ratio was determined using the Y(III)–Arsenazo(III) complex assay (25,31). For radiolabeling, a freshly prepared solution of ascorbic acid (50 μL, 220 μg/ μL) was first added to the ^{86}Y solution (140–170 MBq in 0.1 M nitric acid, 500 μL) to prevent radiolysis of the mAb. The solution was neutralized to pH 5–6 by the addition of ammonium acetate buffer (50 μL 5 M, pH 7.0). CHX-A″-DTPA-Panitumumab (50 μg in 0.15 M ammonium acetate) was added to the mixture, vortexed briefly, and incubated at room temperature for 30 min. The reaction was quenched by the addition of EDTA solution (4 μL, 0.1 M). The radiolabeled product was purified using a PD-10 desalting column (GE Healthcare, Piscataway, NJ, USA). Size exclusion HPLC chromatography using a TSK-3000 column (Toso-Haas,

Montgomeryville, PA, USA) was performed to ascertain the purity of the RIC using previously described solvent conditions and analysis parameters (27).

Cell Lines

HER1-expressing human colorectal (LS-174T), prostate (PC-3) and epidermoid (A431) carcinoma cells (American Type Culture Collection, Rockville, MD, USA) were grown as a monolayer at 37° C, in a humidified atmosphere of 5% CO_2 and 95% air. LS-174T and A431 cells were cultured in Dulbecco's minimal essential medium containing 10% FetaPLEX (Gemini Bio-Products, Woodland, CA, USA) and 10 mM glutamine solution. PC-3 cells were cultured in RPMI-1640 medium containing FetaPLEX (10%). Media and supplements were obtained from Quality Biologicals (Gaithersburg, MD, USA), Invitrogen (Carlsbad, CA, USA) and Lonza (Walkersville, MD, USA).

In vitro evaluations

Radioligand cell-binding studies—The immunoreactivity of the ^{86}Y-CHX-A″-DTPA-panitumumab was determined using a HER1-positive human epidermoid carcinoma A431 fixed-cell radioimmunoassay (RIA) (25).

Animal and tumor models

Female athymic *nu/nu* mice (Charles River Laboratory, Wilmington, MA USA) were injected subcutaneously with 2×10^6 cells of each cell line (200 μL medium containing 20% matrigel, BD Biosciences, Bedford, MA). *In vivo* experiments were performed when the tumor diameter reached 0.5–0.7 cm. Tumor necrosis was examined by Hematoxylin & Eosin (H&E) staining and HER1 expression was confirmed by immunohistochemistry (IHC) on selected formalin-fixed, paraffin-embedded tumors. Tumors were carefully removed and fixed in 4% buffered paraformaldehyde solution and incubated overnight at 4° C. After the incubation period, the fixed tumor was washed with PBS solution and stored in 70% ethanol solution at 4° C before paraffin-embedding. For IHC experiments, panitumumab was used as the primary antibody to determine the available binding sites on the tumor sections. IHC was performed and analyzed at Histoserv, Inc. (Germantown, MD, USA). All animal studies were performed in accordance with the NIH guidelines for the humane use of animals and all procedures were reviewed and approved by the National Cancer Institute Animal Care and Use Committee.

In vivo evaluations

Biodistribution and pharmacokinetic studies—Female athymic mice bearing human colorectal (LS-174T), prostate (PC-3,) or epidermoid (A431) tumor xenografts were injected intravenously (i.v.) via the tail vein with 0.4–0.6 MBq (less than five μg) of ^{86}Y-CHX-A″-DTPA-panitumumab. To determine HER1-specificity, panitumumab (0.1 mg) was co-injected with the radiotracer in an additional set of mice bearing each of the tumor xenografts. At the desired time points, the animals were sacrificed by CO_2 inhalation. Tumor, blood and selected normal organs were harvested, wet-weighed, and the radioactivity was measured in a Wallace Wizard 1480 gamma counter (PerkinElmer, Shelton, CT). The percent injected dose per gram (% ID/g) of tissue was calculated by comparison with standards representing 10% of the injected dose per animal.

Blood pharmacokinetics of the ^{86}Y-CHX-A″-DTPA-panitumumab was determined as previously described (27). The percent-injected dose per mL (% ID/mL) of blood was calculated for each of the samples and clearance determined by biphasic non-linear regression analysis from Graphpad Prism version 5 software (San Diego, CA, USA). Non-compartmental pharmacokinetics was performed to determine AUC, AUMC and the MRT using trapezoidal integration analysis (32).

PET imaging studies—Small animal PET studies were performed using the ATLAS (Advanced Technology Laboratory Animal Scanner) at the National Institute of Biomedical Imaging and Bioengineering, National Institute of Health, Bethesda, MD, USA. Whole body imaging studies (6 bed positions, total acquisition time of 1 h per mouse) were carried out on mice anesthetized with 1.5–1.7% isoflurane on a temperature-controlled bed. Female athymic mice bearing LS-174T, A431 and PC-3 tumor xenografts (n = 3) were injected i.v. with 1.8–2.0 MBq of ^{86}Y-CHX-A″-DTPA-panitumumab. To determine HER1-specificity, excess panitumumab (0.1 mg) was co-injected with the radiotracer. ^{86}Y cylinder phantoms were imaged during each imaging session for normalization and quantitative analysis. The energy window for PET acquisition of ^{86}Y was set between 400 and 700 KeV. The imaging data were reconstructed using 2D-Fourier Rebinned - Ordered Subsets Expectation Maximization method with scatter correction (linear background subtraction). Additional dead time, decay and background corrections were applied for quantitative analysis. The reconstructed images were processed and analyzed using AMIDE (A Medical Image Data Examiner) software program. To minimize spillover effects, regions of interest (ROIs) were drawn to enclose approximately 80–90% of the organ of interest to avoid the edges. To minimize partial-volume effects caused by non-uniform distribution of the radioactivity in the containing volume, smaller ROIs were consistently drawn to enclose the organ. The mice were euthanized and *in vivo* biodistribution studies were performed to determine the correlation between PET-assessed % ID/cc and the *in vivo* biodistribution determined % ID/g.

Statistical Analysis

All numerical data were expressed as the mean of the values ± the standard error of mean (SEM). Graphpad Prism version 5 (San Diego, CA, USA) was used for statistical analysis. A *p* value less than 0.05 was considered statistically significant.

Results

Radiochemistry and *In vitro* evaluations

Modification of panitumumab with the acyclic ligand CHX-A″-DTPA was performed at a 10:1 molar excess of chelate to protein yielding a final chelate to protein ratio of 1.6. The ^{86}Y-CHX-A″-DTPA-panitumumab conjugate was successfully prepared, with the radiochemical yields ranging from 60–75% and specific activity exceeding 2 GBq/mg. The ^{86}Y-CHX-A″-DTPA-panitumumab conjugate demonstrated excellent *in vitro* receptor-specificity as exhibited by an immunoreactivity (%) of 73.51 ± 4.76 and non-specific binding (%) of 3.79 ± 1.69 (n = 4) on fixed A431 cells. On HPLC analysis, the RIC exhibited excellent stability after storage in the refrigerator at 4° C for 1 d and retained the immunoreactivity (Supplemental Figure 1).

In vivo evaluations

Biodistribution studies—In mice bearing LS-174T tumor xenografts, approximately 50% decrease in the blood pool activity was observed over a 4 d time period (14.47 ± 1.28 % ID/g at 1 d to 7.30 ± 1.21 % ID/g at 4 d) (Fig 1A). An opposite trend was observed in tumor uptake, with the % ID/g of 28.43 ± 2.93 observed at 1 d increasing to 34.30 ± 3.47 at 4 d after injection (Fig. 1A). The tumor-to-blood ratio increased more than 2-fold from 2.0 at 1 d to 4.7 at 4 d after injection. In mice bearing PC-3 xenografts, the blood pool activity of the radiotracer decreased from 11.45 ± 0.56 % ID/g at 1 d to 8.66 ± 0.52 % ID/g at 4 d after injection (Fig. 1B). In contrast, approximately 50% increase in the tumor uptake was observed from a 1 to 4 d period (14.53 ± 1.29 % ID/g at 1 d to 27.61 ± 2.81 % ID/g at 4 d after injection). The tumor-to-blood ratios in mice bearing PC-3 xenografts were relatively lower than that observed in mice bearing LS-174T xenografts (1.27 at 1 d after injection to 3.18 at 4 d after injection) because of slower localization of the radiotracer in PC-3 xenografts than the LS-174T xenografts.

The ^{86}Y-CHX-A″-DTPA-panitumumab uptake in all the tumor models was HER1-mediated as demonstrated by the receptor-blocking experiments performed by co-injecting 0.1 mg panitumumab (Fig 2). In mice bearing LS-174T (Fig. 2A), PC-3 (Fig. 2B) or A431 (Fig. 2C) tumors, the tumor % ID/g at 3 d was 34.65 ± 5.9, 22.1± 1.9 and 22.74 ± 1.7, respectively. The corresponding tumor % ID/g in mice co-injected with 0.1 mg panitumumab was 9.28 ± 1.5, 8.80 ± 0.9 and 10.04 ± 1.3, respectively at the same time point, thus demonstrating specificity of the RIC. IHC revealed varied levels of HER1 expression in all tumors. A431 tumors had the highest expression levels of HER1 (Table 1).

Pharmacokinetic analysis—From the blood clearance studies, the $t_{1/2}$ of the α-phase of the biphasic blood clearance ranged from 2.7 ± 1.2 h for mice bearing PC-3 xenografts to 3.7 ± 1.7h for mice bearing LS-174T xenografts (Table 1). The $t_{1/2}$ of the β-phase was identical for all the three tumor models. The mice bearing LS-174T tumor had the highest AUC (96.8 ± 5.6 %ID.d.g^{-1}) and AUMC (262.5 ± 14.9 %ID.d^2.g^{-1}). The tracer accumulation in LS-174T tumors was significantly higher ($p < 0.05$) than A431 and PC-3 tumors as shown in Table 1. However, the tumor MRT were identical for all three tumors (2.7–2.8 d). The LS-174T tumor $AUC_{[0\rightarrow t]}$: blood $AUC_{[0\rightarrow t]}$ ratio of 3.1 was nearly 1.5 times greater than the PC-3 and A431 tumor $AUC_{[0\rightarrow t]}$: blood $AUC_{[0\rightarrow t]}$ ratios of 2.0 (Table 1).

PET imaging studies—The linearity of the PET-assessed concentration *vs*. the radioactivity concentration measured in a Capintec CRC-127R dose calibrator was r^2= 0.99 in the radioactivity range of 0.03–3.63 MBq/mL of ^{86}Y solution from cylindrical phantom studies.

Small animal PET imaging studies were performed in female athymic mice bearing LS-174T (Fig. 3A–B), A431 (Fig. 3C–D) and PC-3 xenograft (Supplemental Figure 2) injected with 1.8–2.0 MBq of ^{86}Y-CHX-A″-DTPA-panitumumab or ^{86}Y-CHX-A″-DTPA-panitumumab co-injected with 0.1 mg panitumumab. The LS-174T (Fig. 3A) and A431 (Fig. 3C) tumors were clearly visualized in maximum intensity projections (top panels) and transverse slices (bottom panels) of mice imaged from 0.5 to 3 d after injection of the RIC. The tumor-to-background ratios improved over the period mostly due to the decrease of radioactivity in blood, liver and background while the tumor uptake increased. In contrast, when 0.1 mg of panitumumab was co-injected with the radiotracer, the tumors were poorly visualized due to receptor-specific blockage, demonstrating the HER1-specificity of ^{86}Y-CHX-A″-DTPA-panitumumab (Fig. 3B and 3D). No significant differences were found in the liver and muscle uptake of mice injected with ^{86}Y-CHX-A″-DTPA-panitumumab and mice co-injected with 0.1 mg cold panitumumab (Fig. 4A). As shown in Fig. 4B, the quantitated tumor uptake of mice injected with ^{86}Y-CHX-A″-DTPA-panitumumab and mice injected with ^{86}Y-CHX-A″-DTPA-Panitumumab + 0.1 mg cold panitumumab were significantly different at 1 d, 2 d and 3 d after injection. However, the tumor uptake were not significantly different at 0.5 d after injection ($p = 0.08$ for LS-174T tumors, $p = 0.10$ for A431 and $p = 0.09$ for PC-3 tumors). For mice bearing LS-174T tumors, the PET assessed tumor $AUC_{[0\rightarrow t]}$ of mice injected with ^{86}Y-CHX-A″-DTPA-Panitumumab was 3.1 times greater than that of mice co-injected with 0.1 mg panitumumab (Table 1). Whereas, the PET assessed tumor $AUC_{[0\rightarrow t]}$ of mice bearing PC-3 and A431 tumors injected with ^{86}Y-CHX-A″-DTPA-Panitumumab were 1.6 and 1.9 times, respectively, greater than that of groups co-injected with 0.1 mg panitumumab. In fact, a statistically significant difference was observed in tumor-bearing mice injected with ^{86}Y-CHX-A″-DTPA-Panitumumab alone and ^{86}Y-CHX-A″-DTPA-Panitumumab co-injected with 0.1 mg panitumumab. The liver, tumor and muscle uptake quantified by PET at all time points were closely related (r^2= 0.95, p= 0.87, n=30) to values determined by *in vivo* biodistribution studies (Fig. 4).

Discussion

Advances in genomics and proteomics are revolutionizing cancer therapy. Significant progress has been made in the development of targeted cancer therapy, wherein the drug specifically targets a unique protein or gene product over-expressed in tumors. Traditionally, *in vitro* assays of tumor biopsy material are used to evaluate the expression of the tumor biomarker that is vital for selecting patients for targeted therapy. Complementary to biopsy assays, molecular imaging has been used to measure regional tumor target expression and therefore select patients for appropriate cancer therapy and to evaluate treatment response (33,34).

Towards this end, ^{86}Y-CHX-A″-DTPA-panitumumab was explored as a non-invasive molecular imaging tool for selecting patients for HER1-targeted panitumumab therapy as well as for dosimetry assessment for possible targeted ^{90}Y therapy.

^{86}Y-CHX-A″-DTPA-panitumumab was routinely prepared with a specific activity exceeding 2 GBq/mg (0.3 GBq/nmol) and radiochemical yields exceeding 60%. When compared to ^{64}Cu-DOTA mAb and ^{89}Zr-Df-mAb, ^{86}Y-CHX-A″-DTPA-mAb offers a viable alternative due to greater *in vivo* stability, greater tumor to background ratios, and significant ease of preparation as demonstrated by this study.

The biodistribution, non-compartmental pharmacokinetics and imaging data reveal HER1-mediated uptake and accumulation in HER1-expressing tumor xenografts (Figure 1–4 and Table 1). The ^{86}Y-CHX-A″-DTPA-panitumumab had relatively longer half-life and slower blood clearance than radiolabeled cetuximab (20). The biodistribution and blood pharmacokinetics of ^{86}Y-CHX-A″-DTPA-panitumumab was similar to ^{111}In-CHX-A″-DTPA-panitumumab, except for lung and femur uptake. These minor differences in ^{111}In and ^{86}Y labeled mAb may be attributed to radiometabolites as previously observed (27). Data on blood clearance and tumor residence time as obtained in this study should prove useful for dosing in panitumumab related therapies.

Studies with ^{64}Cu-DOTA-cetuximab concluded that ^{64}Cu-DOTA-cetuximab could be used to detect and quantify HER1 expression and therefore monitor therapeutic response (22,23). However, no correlation between relative *in vitro* expression determined by flow cytometry, relative *ex vivo* expression determined by IHC and tumor uptake and accumulation (Table 1) was found in the studies presented here. In fact, the cell line (LS-174T) demonstrating the lowest HER1 expression resulted in the highest tumor uptake and accumulation (Table 1 and Figure 1–4). A recent study performed with ^{89}Zr labeled cetuximab also found no correlation between *ex vivo* expression of HER1 and RIC uptake (21). The report describing ^{64}Cu-DOTA-panitumumab also reported discrepancies in tumor uptake and *ex vivo* HER1 expression levels determined by IHC (30). This apparent dichotomy can be explained by the fact that *in vivo* accretion in tumor is actually dependent on many physiological factors including tumor vasculature, blood flow, tumor interstitial pressure, and antigen shedding. Above all else, there is clearly obvious differences between the *in vivo* vs *in vitro* milieu of the surrounding environment ranging from cell-cell interactions to growth factors, etc (35). Therefore, to correlate HER1 expression and tumor uptake further studies are warranted. *In vivo* determination of the distribution of the targeted biomarker and simultaneous determination of its true availability to the drug for therapy provides an extremely important metric that informs on the suitability of the patient for therapy and profoundly personalizes the treatment to the patient. The added advantage is that this information is obtained non-invasively. PET imaging with ^{86}Y-CHX-A″-DTPA-panitumumab may have an extremely useful role in selecting patients for panitumumab related therapy since it would indicate HER1 accessibility to antibody. However, it is also possible that ^{86}Y-CHX-A″-DTPA-panitumumab imaging by itself may not predict the response to therapy as it is only indicative of how much panitumumab

reaches the tumor. It does not reveal the status of KRAS mutations, which is critical for response to HER1 immunotherapy (36–38). Thus, the role of panitumumab imaging may be complimentary and used together with assays to determine KRAS mutations and HER1 gene amplification and polymorphism (36–38).

The available choice of radionuclides used for PET radioimmunoimaging are ^{124}I, ^{64}Cu, ^{89}Zr and ^{86}Y. Each of these radionuclides has their own specific drawback (26). Panitumumab is rapidly internalized, therefore, we anticipate that ^{124}I will be dehalogenated rapidly *in vivo* and result in poor tumor to background ratio. ^{64}Cu-TETA-1A3 has previously been reported for clinical PET imaging of metastatic colorectal cancer (39,40). Although all 17 primary and recurrent sites were clearly visualized in patients, only 23 of 39 metatstatic sites (59 %) were detected (40). Detection of lung and liver metastasis was seriously hindered by non-specific uptake in the liver and the blood due to dissociation of the ^{64}Cu from the currently used chelates for radiolabeling mAbs. ^{89}Zr is an attractive positron emitter due its longer half-life, however preparation of ^{89}Zr labeled mAbs is a multi-step, tedious process and ^{89}Zr has been shown to dissociate from the currently used chelates and to localize in the bone thereafter (24). On the other hand, the chelation chemistry and the preparation of Y labeled mAb for clinical use is well established. While the half-life of ^{86}Y is slightly longer than ^{64}Cu, the abundance of positrons is also almost twice that of ^{64}Cu. With these advantages over ^{64}Cu, we anticipate much lower amounts of ^{86}Y will be required for quantitative immunoPET after 2 d after injection. Based on those previous studies performed with ^{64}Cu labeled mAb (39,40), we anticipate that injection of between 0.18–0.37 GBq of the RIC will result in useful quantitative images up to 2–3 d after injection.

We are currently performing radioimmunotherapy of HER1-expressing solid tumors with ^{90}Y-CHX-A″-DTPA-panitumumab. Therefore, ^{86}Y-CHX-A″-DTPA-panitumumab serves as a surrogate PET marker for dosimetry and selection of subjects for ^{90}Y CHX-A″-DTPA-panitumumab RIT of HER1-expressing carcinoma. To achieve the long-term goal of clinical translation of ^{86}Y-CHX-A″-DTPA-panitumumab, PET/CT and MRI studies are currently being performed with mice bearing orthotopic and disseminated tumors.

Conclusion

In conclusion, ^{86}Y-CHX-A″-DTPA-panitumumab has been prepared with high specific activity. The utility of the RIC for non-invasive PET imaging of HER1-expressing tumors in preclinical models has been demonstrated. ^{86}Y-CHX-A″-DTPA-panitumumab as a radiotracer may be used for the assessment of panitumumab uptake, which may be important for risk stratification, patient screening and appropriate dosage selection. This preclinical study elucidating the biological and pharmacokinetic characteristics of ^{86}Y-CHX-A″-DTPA-panitumumab represents the first step towards the clinical translation.

Supplementary Material

Refer to Web version on PubMed Central for supplementary material.

Acknowledgments

Financial support: The Intramural Research Program of the NIH, NCI, Center for Cancer Research and the United States Department of Health and Human Services.

This research was supported by the Intramural Research Program of the National Institute of Health, National Cancer Institute, Center for Cancer Research and the United States Department of Health and Human Services. Gratitude is expressed to Jurgen Seidel (National Cancer Institute, National Institute of Health, Bethesda, MD) for technical input on the operations of NIH ATLAS small animal PET scanner.

References

1. Hynes NE, Lane HA. ERBB receptors and cancer: the complexity of targeted inhibitors. Nat Rev Cancer 2005;5(5):341–354. [PubMed: 15864276]
2. Burgess AW. EGFR family: structure physiology signalling and therapeutic targets. Growth Factors 2008;26(5):263–274. [PubMed: 18800267]
3. Harari PM. Epidermal growth factor receptor inhibition strategies in oncology. Endocr Relat Cancer 2004;11(4):689–708. [PubMed: 15613446]
4. Mendelsohn J, Baselga J. Epidermal growth factor receptor targeting in cancer. Semin Oncol 2006;33 (4):369–385. [PubMed: 16890793]
5. Patel DD, Goldberg RM. Cetuximab-associated infusion reactions: pathology and management. Oncology (Williston Park) 2006;20(11):1373–1382. discussion 1382, 1392–1374, 1397. [PubMed: 17112000]
6. Messersmith WA, Hidalgo M. Panitumumab, a monoclonal anti epidermal growth factor receptor antibody in colorectal cancer: another one or the one? Clin Cancer Res 2007;13(16):4664–4666. [PubMed: 17699842]
7. Yang XD, Jia XC, Corvalan JR, Wang P, Davis CG. Development of ABX-EGF, a fully human anti-EGF receptor monoclonal antibody, for cancer therapy. Crit Rev Oncol Hematol 2001;38(1):17–23. [PubMed: 11255078]
8. Lynch DH, Yang XD. Therapeutic potential of ABX-EGF: a fully human anti-epidermal growth factor receptor monoclonal antibody for cancer treatment. Semin Oncol 2002;29(1 Suppl 4):47–50. [PubMed: 11894013]
9. Mano M, Humblet Y. Drug Insight: panitumumab, a human EGFR-targeted monoclonal antibody with promising clinical activity in colorectal cancer. Nat Clin Pract Oncol 2008;5(7):415–425. [PubMed: 18506165]
10. Wu M, Rivkin A, Pham T. Panitumumab: Human monoclonal antibody against epidermal growth factor receptors for the treatment of metastatic colorectal cancer. Clin Ther 2008;30(1):14–30. [PubMed: 18343240]
11. Giusti RM, Shastri KA, Cohen MH, Keegan P, Pazdur R. FDA drug approval summary: panitumumab (Vectibix). Oncologist 2007;12(5):577–583. [PubMed: 17522246]
12. Heun J, Holen K. Treatment with panitumumab after a severe infusion reaction to cetuximab in a patient with metastatic colorectal cancer: a case report. Clin Colorectal Cancer 2007;6(7):529–531. [PubMed: 17553202]
13. Nielsen DL, Pfeiffer P, Jensen BV. Six cases of treatment with panitumumab in patients with severe hypersensitivity reactions to cetuximab. Ann Oncol 2009;20(4):798. [PubMed: 19254943]
14. Van Cutsem E, Peeters M, Siena S, et al. Open-label phase III trial of panitumumab plus best supportive care compared with best supportive care alone in patients with chemotherapy-refractory metastatic colorectal cancer. J Clin Oncol 2007;25(13):1658–1664. [PubMed: 17470858]
15. Hecht JR, Patnaik A, Berlin J, et al. Panitumumab monotherapy in patients with previously treated metastatic colorectal cancer. Cancer 2007;110(5):980–988. [PubMed: 17671985]
16. Chung KY, Shia J, Kemeny NE, et al. Cetuximab shows activity in colorectal cancer patients with tumors that do not express the epidermal growth factor receptor by immunohistochemistry. J Clin Oncol 2005;23(9):1803–1810. [PubMed: 15677699]
17. Wen X, Wu QP, Ke S, et al. Conjugation with (111)In-DTPA-poly(ethylene glycol) improves imaging of anti-EGF receptor antibody C225. J Nucl Med 2001;42(10):1530–1537. [PubMed: 11585869]
18. Schechter NR, Wendt RE 3rd, Yang DJ, et al. Radiation dosimetry of 99mTc-labeled C225 in patients with squamous cell carcinoma of the head and neck. J Nucl Med 2004;45(10):1683–1687. [PubMed: 15471833]
19. Barrett T, Koyama Y, Hama Y, et al. In vivo diagnosis of epidermal growth factor receptor expression using molecular imaging with a cocktail of optically labeled monoclonal antibodies. Clin Cancer Res 2007;13(22 Pt 1):6639–6648. [PubMed: 17982120]
20. Milenic DE, Wong KJ, Baidoo KE, et al. Cetuximab: preclinical evaluation of a monoclonal antibody targeting EGFR for radioimmunodiagnostic and radioimmunotherapeutic applications. Cancer Biother Radiopharm 2008;23(5):619–631. [PubMed: 18999934]

21. Aerts HJ, Dubois L, Perk L, et al. Disparity between in vivo EGFR expression and 89Zr-labeled cetuximab uptake assessed with PET. J Nucl Med 2009;50(1):123–131. [PubMed: 19091906]
22. Cai W, Chen K, He L, Cao Q, Koong A, Chen X. Quantitative PET of EGFR expression in xenograft-bearing mice using 64Cu-labeled cetuximab, a chimeric anti-EGFR monoclonal antibody. Eur J Nucl Med Mol Imaging 2007;34(6):850–858. [PubMed: 17262214]
23. Eiblmaier M, Meyer LA, Watson MA, Fracasso PM, Pike LJ, Anderson CJ. Correlating EGFR expression with receptor-binding properties and internalization of 64Cu-DOTA-cetuximab in 5 cervical cancer cell lines. J Nucl Med 2008;49(9):1472–1479. [PubMed: 18703609]
24. Perk LR, Visser GW, Vosjan MJ, et al. (89)Zr as a PET surrogate radioisotope for scouting biodistribution of the therapeutic radiometals (90)Y and (177)Lu in tumor-bearing nude mice after coupling to the internalizing antibody cetuximab. J Nucl Med 2005;46(11):1898–1906. [PubMed: 16269605]
25. Ray G, Baidoo K, Wong K, et al. Preclinical evaluation of a monoclonal antibody targeting the epidermal growth factor receptor as a radioimmunodiagnostic and radioimmunotherapeutic agent. British Journal of Pharmacology 2009;157(8):1541–1548. [PubMed: 19681874]
26. Nayak TK, Brechbiel MW. Radioimmunoimaging with Longer-Lived Positron-Emitting Radionuclides: Potentials and Challenges. Bioconjug Chem 2009;20(5):825–841. [PubMed: 19125647]
27. Garmestani K, Milenic DE, Plascjak PS, Brechbiel MW. A new and convenient method for purification of 86Y using a Sr(II) selective resin and comparison of biodistribution of 86Y and 111In labeled Herceptin. Nucl Med Biol 2002;29(5):599–606. [PubMed: 12088731]
28. Palm S, Enmon RM Jr, Matei C, et al. Pharmacokinetics and Biodistribution of (86)Y-Trastuzumab for (90)Y dosimetry in an ovarian carcinoma model: correlative MicroPET and MRI. J Nucl Med 2003;44(7):1148–1155. [PubMed: 12843231]
29. Helisch A, Forster GJ, Reber H, et al. Pre-therapeutic dosimetry and biodistribution of 86Y-DOTA-Phe1-Tyr3-octreotide versus 111In-pentetreotide in patients with advanced neuroendocrine tumours. Eur J Nucl Med Mol Imaging 2004;31(10):1386–1392. [PubMed: 15175836]
30. Niu G, Li Z, Xie J, Le QT, Chen X. PET of EGFR Antibody Distribution in Head and Neck Squamous Cell Carcinoma Models. J Nucl Med 2009;50(7):1116–1123. [PubMed: 19525473]
31. Pippin CG, Parker TA, McMurry TJ, Brechbiel MW. Spectrophotometric method for the determination of a bifunctional DTPA ligand in DTPA-monoclonal antibody conjugates. Bioconjug Chem 1992;3(4):342–345. [PubMed: 1390990]
32. Gibaldi, M.; Perrier, D. Pharmacokinetics. 2. New York: Dekker; 1982.
33. Zhao B, Schwartz LH, Larson SM. Imaging surrogates of tumor response to therapy: anatomic and functional biomarkers. J Nucl Med 2009;50(2):239–249. [PubMed: 19164218]
34. Mankoff DA. Molecular imaging to select cancer therapy and evaluate treatment response. Q J Nucl Med Mol Imaging 2009;53(2):181–192. [PubMed: 19293766]
35. Horan Hand P, Colcher D, Salomon D, Ridge J, Noguchi P, Schlom J. Influence of spatial configuration of carcinoma cell populations on the expression of a tumor-associated glycoprotein. Cancer Res 1985;45(2):833–840. [PubMed: 3881173]
36. Di Nicolantonio F, Martini M, Molinari F, et al. Wild-Type BRAF Is Required for Response to Panitumumab or Cetuximab in Metastatic Colorectal Cancer. J Clin Oncol 2008;26(35):5705–5712. [PubMed: 19001320]
37. Amado RG, Wolf M, Peeters M, et al. Wild-type KRAS is required for panitumumab efficacy in patients with metastatic colorectal cancer. J Clin Oncol 2008;26(10):1626–1634. [PubMed: 18316791]
38. Jimeno A, Messersmith WA, Hirsch FR, Franklin WA, Eckhardt SG. KRAS mutations and sensitivity to epidermal growth factor receptor inhibitors in colorectal cancer: practical application of patient selection. J Clin Oncol 2009;27(7):1130–1136. [PubMed: 19124802]
39. Cutler PD, Schwarz SW, Anderson CJ, et al. Dosimetry of copper-64-labeled monoclonal antibody 1A3 as determined by PET imaging of the torso. J Nucl Med 1995;36(12):2363–2371. [PubMed: 8523133]

40. Philpott GW, Schwarz SW, Anderson CJ, et al. RadioimmunoPET: detection of colorectal carcinoma with positron-emitting copper-64-labeled monoclonal antibody. J Nucl Med 1995;36(10):1818–1824. [PubMed: 7562049]

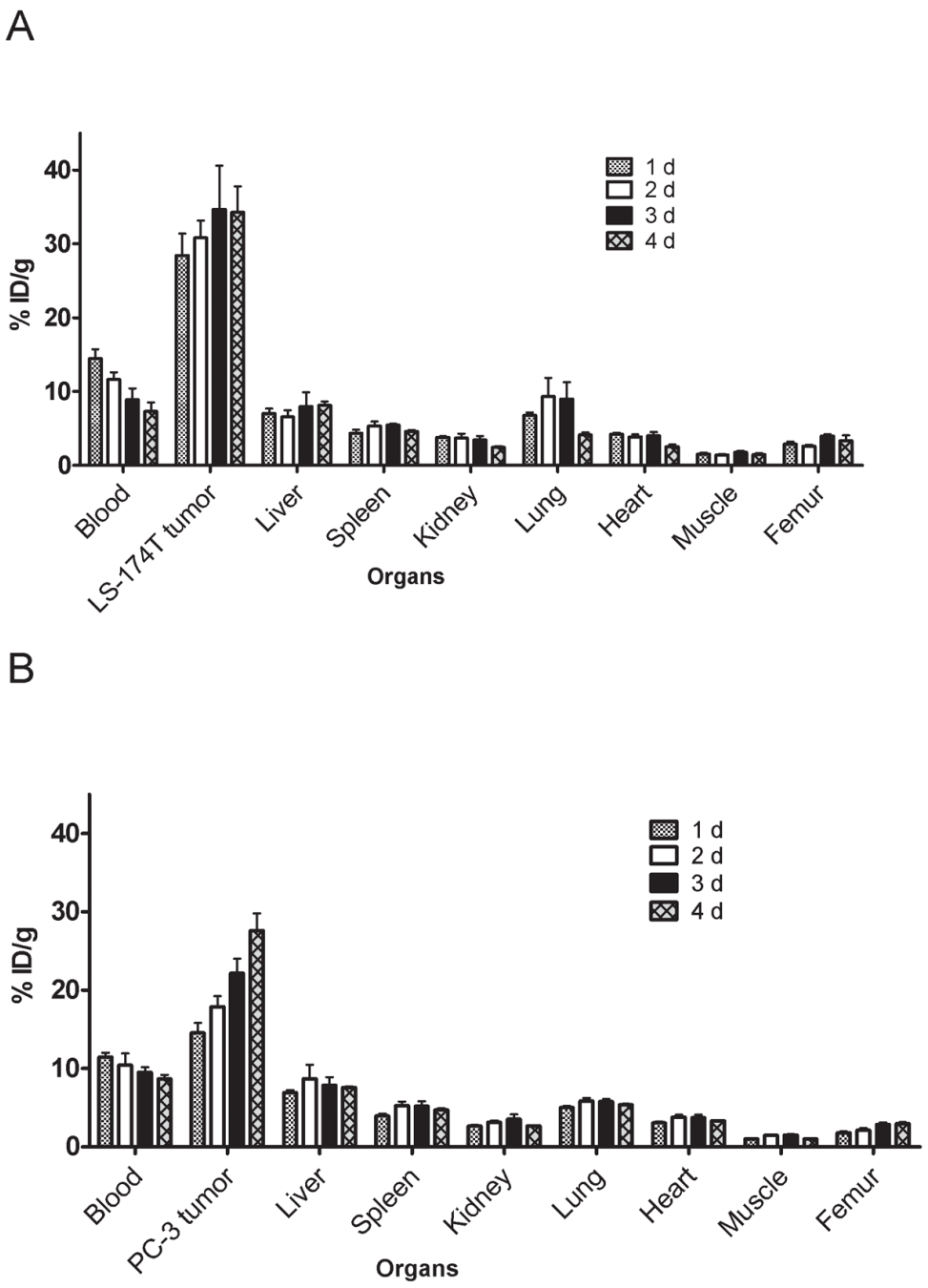

Figure 1.

Biodistribution of ^{86}Y-CHX-A″-DTPA-panitumumab in selected organs of female athymic (NCr) *nu/nu* mice bearing human colorectal carcinoma LS-174T **(A)** and human prostate carcinoma PC-3 **(B)** tumor xenografts. Biodistribution data were obtained at 1, 2, 3 and 4 d after i.v. injection of ^{86}Y-CHX-A″-DTPA-panitumumab. All values are expressed as % ID/g. Data represent the mean value ± SEM from at least four determinations.

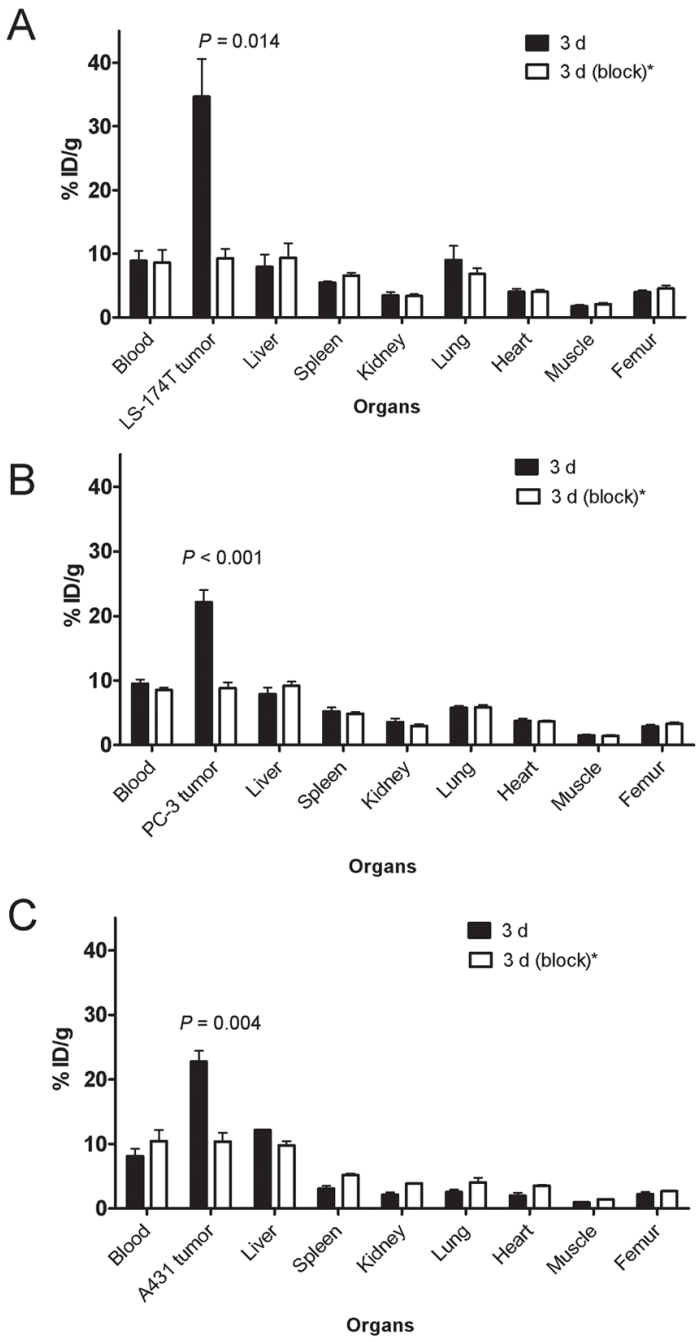

Figure 2.

Receptor-meditated uptake of ^{86}Y-CHX-A″-DTPA-panitumumab in selected organs of female athymic (NCr) *nu/nu* mice bearing human colorectal carcinoma LS-174T **(A)**, human prostate carcinoma PC-3 **(B)** and human epidermoid carcinoma A431 tumor xenografts **(C)**. Biodistribution data were obtained at 3 d after injection. All values are expressed as % ID/g. Data represent the mean value ± SEM from at least three determinations.

*Receptor blocking studies were performed by co-injecting 0.1 mg panitumumab with the radiotracer.

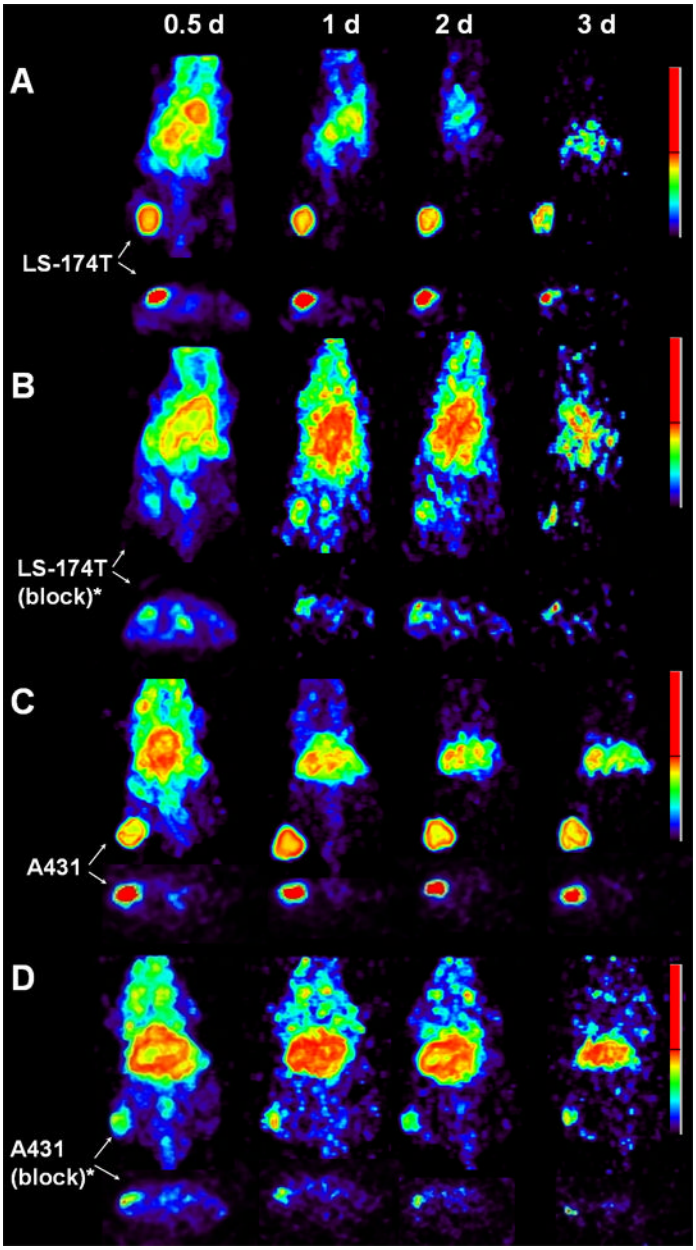

Figure 3.

Representative reconstructed and processed maximum intensity projections (top panel) and transverse slices (bottom panel) of female athymic (NCr) *nu/nu* mouse bearing human colorectal carcinoma LS-174T (3A and 3B) and human epidermoid carcinoma A431 tumor xenografts (3C and 3D). Mice represented in 3A and 3C were injected i.v. via tail vein with 1.8–2.0 MBq of ^{86}Y-CHX-A″-DTPA-panitumumab, and mice represented in 3B and 3D were co-injected i.v. via tail vein with 1.8–2.0 MBq of ^{86}Y-CHX-A″-DTPA-panitumumab and 0.1 mg Panitumumab for blocking HER1. The tumors are indicated with a white arrow. The scale represents % maximum and minimum threshold intensity.

*Receptor blocking studies were performed by co-injecting 0.1 mg panitumumab with the radiotracer.

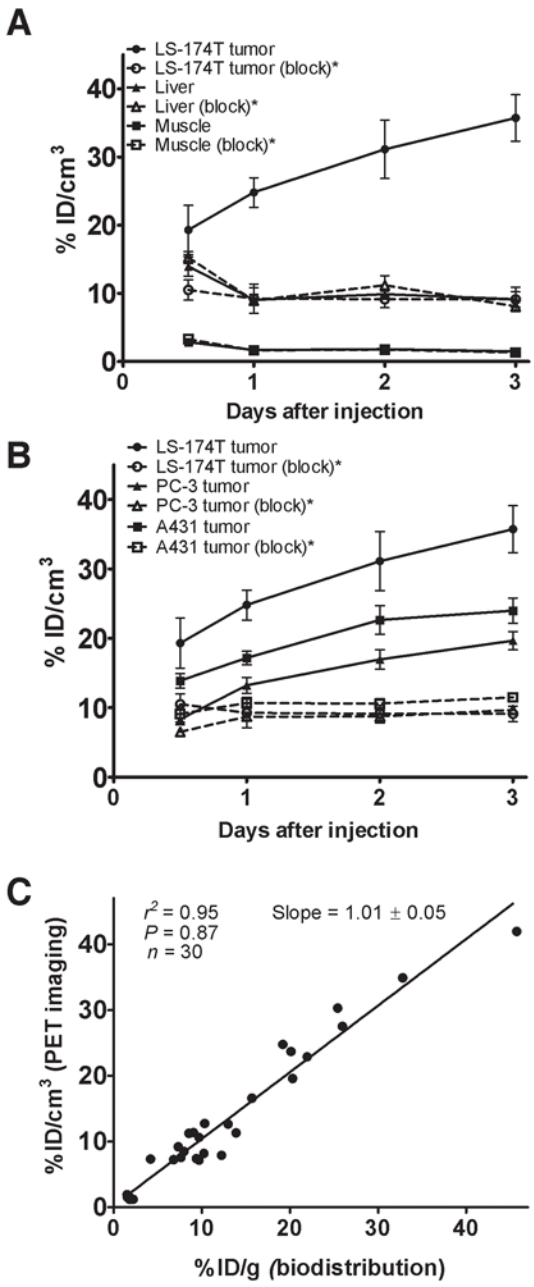

Figure 4.

(A) Time-activity curve and uptake values of ^{86}Y-CHX-A″-DTPA-panitumumab in selected organs of female athymic (NCr) *nu*/*nu* mice bearing human colorectal carcinoma LS-174T xenografts assessed through quantitative small animal PET imaging. **(B)** Comparative time-activity curves of ^{86}Y-CHX-A″-DTPA-panitumumab in female athymic (NCr) *nu*/*nu* mice bearing LS-174T, A431 and PC-3 tumor xenografts. **(C)** Correlation between organ % ID/g values assessed through *in vivo* biodistribution studies and quantitative small animal PET imaging. All uptake values derived from PET studies are expressed as % ID/cc. Data represent the mean value ± SEM from three determinations.

*Receptor blocking studies performed by co-injecting 0.1 mg panitumumab with the radiotracer.

Table 1

Pharmacokinetic characteristics of ^{86}Y-CHX-A″-DTPA-panitumumab injected i.v. via tail vein of female athymic (NCr) *nu*/*nu* mice bearing LS-174T, PC-3 and A431 tumor xenografts. Data represent the mean values from three to six determinations.

Pharmacokinetic characteristics	LS174T (Colorectal)	PC-3 (Prostate)	A431 (Epidermoid)
Relative *in vitro* expression[#]	62.5	150.9	2072.2
Relative *in vivo* expression	+	+−++	+++
Blood clearance (h)			
α-$t_{1/2}$	3.7 ± 1.7	2.7 ± 1.2	3.1 ± 1.3
β-$t_{1/2}$	58.4 ± 15.3	69.2 ± 14.4	73.9 ± 13.0
Blood $AUC_{[0\rightarrow4]}$ (%ID.d.g^{-1})	31.4 ± 1.5	30.0 ± 2.2	32.3 ± 2.2
Tumor $AUC_{[0\rightarrow4]}$ (%ID.d.g^{-1})	96.8 ± 5.6	61.1 ± 3.7	65.3 ± 3.2
Tumor PET $AUC_{[0\rightarrow3]}$ (%ID.d.cc^{-1})	72.4 ± 5.3	38.8 ± 2.8	51.2 ± 2.9
Tumor PET $AUC_{[0\rightarrow3]}$ (%ID.d.cc^{-1})[*]	23.2 ± 3.7	21.7 ± 1.0	26.3 ± 1.9
Tumor $AUC_{[0\rightarrow4]}$: Blood $AUC_{[0\rightarrow4]}$	3.1	2.0	2.0
Tumor $AUMC_{[0\rightarrow4]}$ (%ID.d^2.g^{-1})	262.5 ± 14.9	171.9 ± 10.3	179.9 ± 8.8
Tumor MRT (d)	2.7	2.8	2.7

[#]Mean fluorescence intensity from flow cytometry cell binding studies as a measure of relative *in vitro* expression. Data adapted from Ray GL et al. (41).

[*]Receptor blocking studies performed by co-injecting 0.1 mg panitumumab with the radiotracer. Values obtained from the blocking studies were significantly lower than the unblocked studies ($p < 0.05$) demonstrating receptor-mediated accumulation in the tumors.